processes

MDPI

Article

Binderless Hardwood Tree Bark-Based Insulation Panels for Green Building Applications

Volha Mialeshka * and Zoltán Pásztory

Faculty of Wood Engineering and Creative Industries, University of Sopron, 4 Bajcsy Zs. Str., 9400 Sopron, Hungary; pasztory.zoltan@uni-sopron.hu
* Correspondence: mialeshkavolha@phd.uni-sopron.hu

Abstract

Tree bark, an abundant by-product of the timber industry, represents a promising feedstock for sustainable construction. This study investigates the thickness swelling, water absorption, hygroscopicity and mechanical (compressive strength) properties of insulation panels produced from hardwood bark (*Tilia* spp. and *Robinia pseudoacacia*) via hydromechanical treatment and a wet-forming process. The panels were produced without added adhesives, relying on the formation of hydrogen bonds during the drying phase to ensure structural integrity. Both bark-based insulation boards (thermal conductivity coefficient 0.055–0.057 W/m·K) showed similar hygroscopic behavior, reaching equilibrium moisture contents of max. 25% at 93.9% RH. Water absorption after 24 h immersion was highly material-dependent; *Tilia*-based panels showed 57.11 ± 5.81%, and *Robinia*-based panels 320.61 ± 11.34%. Thickness swelling remained low (max. 6% for *Robinia*), showing significant orthotropic anisotropy. At 10% compressive strain, the *Tilia* and *Robinia* bark-based panels showed compressive strengths of 188 ± 14.6 kPa and 298 ± 18.1 kPa, accordingly. These findings demonstrate that hardwood bark can be successfully valorized into high-performance, binderless insulation, supporting circular economic strategies.

Keywords: tree bark; thermal insulation; sustainable construction; bio-based materials; circular economy; wet-forming process; *Robinia pseudoacacia*; *Tilia* spp.

1. Introduction

1.1. Global Context

Anthropogenic GHG (greenhouse gas) emissions contribute to global warming and increase the risk of persistent and widespread food insecurity and malnutrition, especially among vulnerable population groups [1]. The construction sector is one of the largest contributors to climate change, accounting for significant emissions due to the fossil-fuel-intensive production of materials and high energy consumption during building operations [2,3]. Reducing both operational and embodied energy requires a fundamental transition toward sustainable building materials. Investment in thermal insulation offers a "triple win" (economic, environmental, and social) and is a central element of sustainable construction, especially for aging building stocks with poor thermal performance [4]. While the transition toward natural materials and industrial by-products aligns with circular economy principles, the return to bio-based sources must be managed carefully. It should not be assumed that natural materials automatically result in carbon neutrality [5]. Every production step requires energy input, which impacts the total CO_2 emissions associated

Academic Editors: Artur Spat Ruviaro, Laura Silvestro and Henrique Almeida Santana

Received: 13 March 2026
Revised: 22 April 2026
Accepted: 29 April 2026
Published: 30 April 2026

with the material's life cycle [6]. Predictive models for time, cost, energy, and emissions are essential at early development stages to ensure true sustainability [7].

1.2. Conventional vs. Natural-Based Insulation Materials

Materials such as mineral and glass wool, petroleum-based foams (polystyrene, polyurethane, phenolic), perlite or aerated concrete are market-dominant due to their efficiency and low cost. However, they are based on non-renewable resources, contain toxic additives, and pose significant recycling challenges [8].

Bio-based alternatives derived from wood by-products, recycled paper, hemp, or agricultural waste offer renewable and biodegradable solutions [9]. At the same time, wood fiber- and grass-based insulation has a much more advantageous carbon footprint than that of EPS (expanded polystyrene) and mineral wool [10].

Conventional insulation materials typically achieve thermal conductivity values between 0.028 and 0.034 W/(m·K) [11]. Recent advancements show that natural fibers like hemp, flax, and straw can reach competitive ranges of 0.034–0.046 W/(m·K), while bio-based aerogels can drop below 0.025 W/(m·K) [12]. However, to compensate for the embodied CO_2 of other components in case of timber and bamboo structures, bio-based insulation may require thicknesses of up 0.58–1 m [13]. A key advantage of natural materials is their high vapor permeability, which enables moisture buffering and improves indoor air quality [14]. Compared to expanded polystyrene (EPS), bio-based materials can be up to three times more vapor-permeable [15]. Hygroscopicity is a critical parameter to characterize bio-based building materials because it directly dictates the durability, thermal performance, and moisture buffering capacity. Key methods include determining the moisture sorption isotherm, calculating the dynamic moisture buffer value (MBV), and assessing pore structure [16,17].

The mechanical performance of bio-based materials is categorized by their density and structural application into hard and soft materials. The mechanical behavior is characterized by anisotropy (properties varying based on the direction of the fibers) and is heavily influenced by the material's mass density [9]. In the case of natural material-based composites, with increasing amounts of fibers, the material becomes more porous, which reduces the density and makes materials more brittle, showing lower compressive strength [18,19].

The primary challenge of natural-based insulation remains durability, which can be addressed through surface treatments or nanoparticle reinforcement [20].

1.3. Potential of Tree Bark in Thermal Insulation

Tree bark constitutes approximately 10–12% of a log's volume and is a primary by-product of the timber industry. Currently, bark is largely utilized for energy recovery (burning) or the extraction of tannins and polyphenols; however, it is also used for the development of high-value composite materials [21,22].

Historically, bark fibers have already been investigated for papermaking [23], demonstrating their potential in panel production across various formats, including whole pieces, particles, and fibers [24], even when sourced from insect-damaged trees [25] or used as loose-fill insulation [26]. Research on Southeast Asian *Gelam* wood bark particles pressed at 128 °C showed physical properties meeting Indonesian standards for particleboards [27]. Some studies suggest that bark boards produced with MUF (melamine urea formaldehyde) adhesives may exhibit lower mechanical performance compared to wood chip boards but offer superior thermal insulation [28]. For instance, spruce bark fiber boards achieved thermal conductivity values of 0.044 W/(m·K) [29], while eucalyptus bark fibers ranged from 0.036 to 0.059 W/(m·K) depending on density (80–220 kg/m^3) and binder type [30]. Mechanical properties like Internal Bond (IB), Modulus of Rupture (MOR), and Modulus of

Elasticity (MOE) are highly dependent on particle orientation and density [31]. For example, bark-based panels with a density of 500 kg/m^3 have reached an MOR of 2.94 N/mm^2 and an MOE of 502 N/mm^2 [32].

1.4. Research Rationale and Objectives

In studies of thermal insulation materials, softwood species such as spruce and larch predominate, while hardwood species are less represented, specifically *Tilia* spp. (lime) and *Robinia pseudoacacia* (black locust), indicating a gap in the literature. Softwood species provide a lower thermal conductivity (0.044 to 0.063 W/(m·K)) [29], while hardwood species, for example, gelam, demonstrate significantly higher thermal conductivity 0.14 W/(m·K) [33]. This is explained by the morphology of the fibers and the lower density of coniferous bark. In questions of moisture resistance, hardwood species (oak) show stability with swelling at a thickness of about 10%, while in conifers this range is wider, from 10% to 30% [34]. However, deciduous species, such as eucalyptus, can reach extremely low thermal conductivity values (0.036 W/(m·K)) with deep chemical and mechanical processing [30]. Conifers are more often used for thermal insulation because of their availability, porous structure and self-adhesion ability in wet production without synthetic resins. The use of hardwood species is limited by their high variability of density and the difficulty of extracting high-quality fiber, which requires additional processing stages, such as alkaline cooking.

While existing studies have primarily focused on panels produced through air-laid techniques [35] or hot-pressing methods [34], this study aims to evaluate the mechanical and hygrothermal properties of hardwood (*Robinia pseudoacacia* and *Tilia* spp.) bark panels fabricated via a hydromechanical wet-forming process. This wet-processing approach is underrepresented in the literature, but highly advantageous as it facilitates the production of binderless, self-bonding panels, which makes the material recyclable and significantly reduces the environmental impact associated with chemical additives still used for fiber board production.

The novelty of this study lies in the investigation of the performance (hydroscopic and mechanical properties) of insulation panels made from hardwood bark using a wet-processing method without any adhesives. The scope of this study includes the determination of compressive strength, thickness swelling, moisture content, and moisture solubility, which represents a valuable addition to existing data. In our previous experimental work, bark-based panels made of *Tilia* spp. and *Robinia pseudoacacia* showed thermal conductivity [36] ranging from 0.055 to 0.057 W/m·K. These values indicate high potential for further testing of eco-friendly thermal insulation materials and reasonable consideration of them as an alternative to traditional insulation materials.

2. Materials and Methods

2.1. Material Preparation and Board Formation

Binderless insulation panels were fabricated using bark from *Robinia pseudoacacia* (black locust) and *Tilia* spp. (European lime). The barks were collected from a sawmill in the Bakony mountains (Hungary). The production process was carried out according to the methodology described in our previous work [36]. Specifically, raw bark (Figure 1a) was milled using a 12 mm sieve. Following this, the bark particles were immersed in water and refined using a laboratory refiner (Valmet Oyj, Espoo, Finland). The resulting pulp was poured into a circular mold for mat formation. After dewatering, the samples were placed in a drying chamber for 3–5 days at 60 °C (Figure 1b). The resulting boards (Figure 1c) had a thickness of 47 mm and a diameter of 50 cm. Mean densities are 218 ± 4 kg/m^3 for *Tilia* spp. (lime bark insulation panel—LIP) and 231 ± 9 kg/m^3 for *Robinia pseudoacacia* (black locust insulation panel—BIP), where ± represents the standard deviation. Post-defibration fiber lengths ranged from 0.2 to 4.5 mm, with a primary fraction of 0.2–0.5 mm; fiber widths ranged from 0 to 80 μm [36].

Figure 1. Material processing stages: (**a**) raw bark prior to impact milling; (**b**) milled bark prior to immersion and defibration; (**c**) dried panels after sanding and prior to testing (BIP on the top, LIP on the bottom).

2.2. Testing Methods

2.2.1. Hygroscopic Sorption

Hygroscopic behavior of the insulation panels was evaluated in accordance with ISO 12571:2021 [37] using the desiccator method. Cubic specimens (20 × 20 × 20 mm^3) were dried to constant mass at 105 °C. Overall, 10 samples of each material type (total n = 20) were used per desiccator.

After reaching constant weight, the samples were placed into six desiccators, each maintained at a controlled relative humidity (φ) via saturated salt solutions. The actual average RH for the six desiccators was 15, 34, 48, 70, 82, and 91% respectively. Equilibrium moisture content (u) was determined upon mass stabilization using Equation (1):

$$u = \frac{m - m_0}{m} \times 100 \quad (1)$$

where m is the equilibrium mass (g) of the wet sample and m_0 is the oven-dried sample mass (g). The relationship between u and φ is graphically represented in the sorption isotherm for each specific panel (Figure 2).

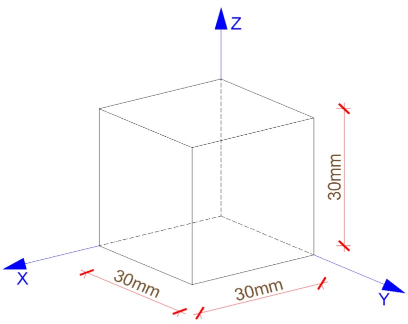

Figure 2. Schematic representation of the specimen geometry (30 × 30 × 30 mm^3) for thickness swelling measurements. Arrows along the X, Y, and Z axes indicate the directions of measurement of the linear dimensions used to calculate swelling in three directions.

2.2.2. Thickness Swelling and Water Absorption Measuring

Thickness swelling (TS) was measured according to EN 317:1993 [38]. Water absorption (WA) was determined per ASTM C1763-20 [39]. A total of 32 specimens (30 × 30 × 30 mm^3) were tested, with 16 replicates per material type. To ensure the repeatability of the results and account for potential material heterogeneity, specimens were obtained from four independent panels (two per material). From each panel, eight specimens were selected using a systematic random sampling method. Both TS and WA were measured concurrently on the same set of specimens after a 24 h immersion period.

Measurements of TS were taken across three planes: perpendicular to the plane (Z axis) and parallel to the plane (X and Y axes) (Figure 2).

Thickness swelling in the direction parallel to the plane was calculated as the arithmetic mean of the measurements along the X and Y axes. Thickness swelling was calculated as (2)

$$TS = \frac{t_2 - t_1}{t_1} \times 100 \quad (2)$$

where t_1 is the thickness before immersion (mm) and t_2 is the thickness after immersion (mm).

Water absorption by weight was calculated as (3)

$$WA = \frac{W_2 - W_1}{W_1} \times 100 \quad (3)$$

where W_1 is the pre-immersion weight (g) and W_2 is the weight after immersion, draining, and blotting (g).

2.2.3. Compressive Properties

The compressive strength was tested with some modification to EN 826:2013 [40] using 5985 Universal Testing Machine (Instron, Norwood, MA, USA).

For each material type, two panels were produced. A total of n = 64 cubic specimens (30 × 30 × 30 mm^3) were prepared for the study. From each panel, 16 specimens were selected using a systematic random sampling method. Prior to testing, all specimens were conditioned at 23 °C ± 2 °C and 50% ± 5% RH for 24 h. Testing was performed in two loading directions relative to the panel orientation: parallel and perpendicular to the panel surface. For each material type, 16 specimens were tested per loading direction.

Loading was applied at a rate of 3 mm/min until 10% deformation. Compressive strength at 10% deformation (σ_{10}) (4) and maximum compressive strength (σ_{max}) (5) were calculated as follows:

$$\sigma_{10} = \frac{F_{10}}{A_0} \quad (4)$$

$$\sigma_{max} = \frac{F_{max}}{A_0} \quad (5)$$

where F_{10} is the force at relative 10% deformation (N), F_{max} is the maximum force (N), and A_0 is the initial cross-sectional area of the specimen (mm^2).

Young's modulus (E) was calculated as (6):

$$E = \frac{\Delta F \times L_0}{A_0 \times \Delta L} \quad (6)$$

where ΔF is the change in applied load between two selected points on the elastic linear region of the curve (N), A is the cross-sectional area of the specimen (mm^2), ΔL is the change in the specimen's height (deformation) corresponding to the force ΔF (mm), and L_0 is the length of the specimen before applying compression load [41].

2.2.4. Thermal Conductivity

The thermal insulation performance was evaluated following ISO 8301 [42] /EN 12667 [43] standards using a steady-state heat flow meter. Tests were performed on samples with a 45 cm diameter and 47 mm thickness, maintaining a constant temperature difference of 10 °C (5 °C cold side, 15 °C warm side). The thermal conductivity coefficient (λ) was calculated based on the one-dimensional heat flow in Equation (7), with results averaged over 100 data points after reaching steady-state conditions.

$$\lambda = \frac{q}{\frac{dT}{dx}} \quad (7)$$

2.3. Statistical Analysis

To assess the significance of experimental factors and quantify intergroup differences in the physical and mechanical properties of the studied materials, Linear Mixed-Effects Models (LMMs) were applied to perform Mixed-Effects Analysis of Variance (ANOVA). In all models, material and, where applicable, loading or thickness swelling direction (parallel vs. perpendicular) were treated as fixed factors, including their interaction terms [44]. Panel (Batch) was included as a random effect. To solve observed heteroscedasticity, models were balanced using a variance function (varIdent) to assign for group-specific variances. Standard assumptions (normality of residuals and homoscedasticity) were verified via Shapiro–Wilk tests, Q–Q plots, and Levene's tests. Post hoc comparisons were conducted using Tukey or Bonferroni adjustments, with effect sizes reported as Partial Omega Squared. All statistical analyses were performed using RStudio (Version 2025.09.2, Build 418) with the R programming language. Full ANOVA tables are provided in the Supplementary Materials.

3. Results and Discussion

3.1. Hygroscopic Sorption Behavior

The sorption isotherms for the BIP and LIP (see Figure 3) demonstrate the typical hygroscopic behavior of lignocellulosic materials (type II isotherm) [45], characterized by a non-linear increase in moisture content with relative humidity. Both materials exhibit a relatively linear moisture uptake until approximately 50% RH. In this range, water molecules bind to the internal pore surfaces via hydrogen bonding or Van der Waals forces, forming a monomolecular layer. Between 70% and 80% RH, a slight plateau or "straight section" indicates the saturation of primary adsorption sites and the onset of polymolecular layer formation. Beyond 80% RH, MC increases exponentially caused by capillary condensation. According to the Kelvin equation, reduced vapor pressure over curved menisci ensures that pores of a specific radius fill with liquid water at a given RH [45]. These results align with findings by Petcu et al. [46] for cardboard and cellulose waste, which remained stable until 75% RH. At 90% RH and above, these materials showed rapid growth that exceeded the levels observed for polystyrene [47].

LIP showed a higher sorption capacity than BIP above 50% RH. At 93.9% RH, LIP reached approximately 25% MC compared to 21.4% for BIP, likely due to the high degree of porosity of the material. The MC values for both materials at high RH are comparable to wood fibers, which can exceed 25% at 90% RH [48], and are notably higher than the 18.7% reported for *C. obtusa* (French Guiana species) bark fiber-based insulation materials [35].

The high moisture fixation capacity of bio-based materials directly impacts thermal efficiency. Petcu et al. [46] in the study showed that a 1% increase in MC can elevate the thermal conductivity (λ) by 1.25–2%. Fibrous materials are sensitive to significant increases in thermal conductivity when wet; in some cases, a 2–3% (vol. %) increase in moisture content can increase λ by more than 2.5 times due to the formation of "water bridges" between the fibers [49].

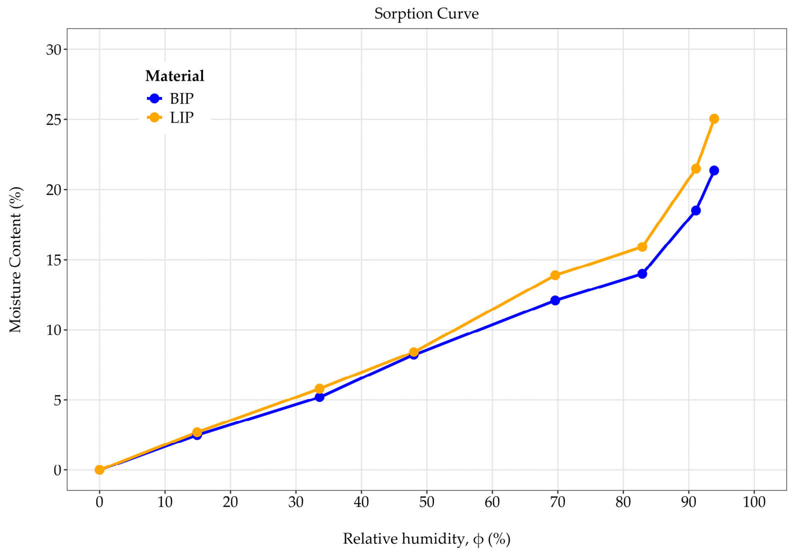

Figure 3. Sorption isotherms obtained for BIP and LIP. Data points mark equilibrium measurement points.

Good hygroscopic properties also allow these materials to function as effective moisture regulators. The speed of vapor movement through pores is often more critical to building health than the maximum water capacity [48]. In this study, at higher humidity levels (>80% RH), the materials reached 50–80% of their total moisture capacity within the first 24–48 h. While initial water uptake was rapid, the panels did not reach full equilibrium even after 10 days of observation. For dense bark structures, as presented in [35], the "slow-saturation" behavior showed a beneficial "buffer effect" for indoor climate regulation

It should be noted that the results presented in this study reflect the potential sorption capacity of the materials, rather than the full cyclic profile of the moisture buffer value (MBV), which is strongly influenced by adsorption/desorption hysteresis. Porous materials such as bio-based materials (hemp, wood) retain more moisture during desorption than they can adsorb at the same relative humidity [50]. However, for practical construction applications of natural-based materials, sorption kinetics may be more significant than static hysteresis. Ranefjard et al. [48] showed that despite differing isotherms and hysteresis widths, wood fiber, grass, and seagrass exhibit similar MBV performance.

Materials that retain moisture due to the desorption hysteresis effect create a favorable environment for microorganisms [46].

Although this study was not primarily designed to evaluate biostability, visual signs of mold were detected during sorption testing. Specifically, mold growth appeared after incubation in a desiccator at 90% relative humidity, which corresponds to a material moisture content of approximately 20%. At these humidity levels, untreated biomaterials are vulnerable to fungi and insects, which prevent their effective use in construction [9]. Strategies for protecting these materials include environmental humidity control and active air circulation, natural antimicrobial additives (essential oils, chitosan, propolis), which can be incorporated into the material matrix or applied as functional coatings [51], or thermomechanical processing and alkali pretreatment (4% NaOH) [52]. The use of biocompatible, breathable coatings, such as lime or clay mortars, can preserve the material's natural moisture-buffering properties without the risk of critical moisture accumulation [47].

3.2. Thickness Swelling and Water Absorption

The dimensional stability of LIP and BIP demonstrated an orthotropic swelling pattern, reflecting the material's tendency to increase in volume at different rates along three mutually perpendicular axes. Statistical analysis confirmed that thickness swelling (TS) in the perpendicular direction (Z) is significantly higher ($p < 0.001$) than in the parallel directions (X, Y) for both panel types (Figure 4).

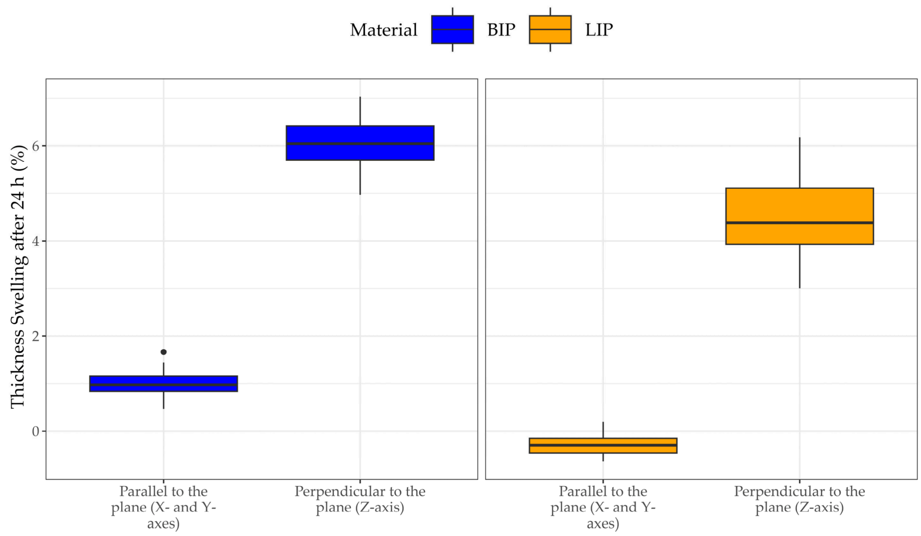

Figure 4. Thickness swelling anisotropy by sample direction for BIP and LIP samples.

This anisotropy is likely caused by the preferential horizontal orientation of defibrated fibers during gravitational sedimentation as water was removed during the wet-forming process. When elongated fibers settle in a liquid medium, their behavior is governed by an interplay of gravitational force, buoyancy, and viscous resistance [53]. Under slow sedimentation, particles tend to settle into a predominantly horizontal orientation relative to the vertical axis of the forming mat [54]. During the drying phase, surface tension forces pull the fibers into tight closeness, causing transverse contraction. When the material is subsequently exposed to water, it tends to "expand" primarily in the direction of its original compression (i.e., along the panel thickness) [55]. This mechanism remains a theoretical assumption within the scope of the present study. Direct verification of fiber alignment X-ray micro-computed tomography (micro-CT) or advanced microscopic analysis are required to provide definitive structural evidence.

According to the EN 622-4 [56] standard, the manufactured bark fiber panels (218–231 kg/m^3) are classified as softboards. However, their exceptional dimensional stability, with a TS of only 4.5–6.04% after 24 h of immersion, exceeds the requirements for the moisture resistance of softboards. In contrast, dry-processed wood-based panels have reported TS values as high as 60% [57] using urea–formaldehyde (UF) or polymeric diphenylmethane diisocyanate (pMDI) as a binder. In other study, wet-processed insulation materials derived from softwood bark fibers showed a TS of max 25% [29].

Statistically significant differences in water absorption (WA) were observed between materials ($p < 0.001$, ANOVA and Tukey's post hoc test). BIP exhibited significantly higher WA (320.61 $\pm$ 11.58%) compared to LIP (57.11 $\pm$ 9.23%). A significant variation between two produced boards of the same material was also identified; this discrepancy may be due to slight differences in pressing conditions, as the panels were formed under gravity and water pressure during mat formation. Visually (Figure 5), it can be seen that the LIP samples remained more cohesive and drier inside, while the BIP samples showed minor delamination and were highly saturated with moisture.

https://doi.org/10.3390/pr14091450

(a) (b)

Figure 5. Material after 24 h of complete immersion in water. LIP (**a**) and BIP (**b**) samples after immersion in water. Samples were hand-damaged for the visualization.

This behavior is attributed to the lower density of certain specimens and the higher fiber fraction in lime bark, which creates a more intricate fiber network [36]. Upon immersion, fiber swelling and capillary action transport water molecules along the fiber–matrix interface, followed by the leaching of water-soluble substances. This process resulted in a pH shift from 7.5 to 8.0 for LIP and 7.5 to 8.2 for BIP prior to delamination [58]. Similar trends have been noted in softwood bark panels, where WA values ranged from 55% to 380% [29].

3.3. Compressive Strengths

At 10% deformation (3 mm), BIP is 65.4% stronger in parallel (to the panel surface) and 59.6% stronger perpendicular than lime ($p < 0.01$). A Two-Way ANOVA was applied (Figure 6). The residual standard error of the model was approximately 20 kPa, which is significantly lower than the observed difference between species. The unevenness of the panel density is manifested in the scatter of individual measurements (gray dots in Figure 6) with a coefficient of variation (CV) of less than 10.6%. Specimens were taken from different sections without density correction. Density within the panels is distributed non-uniformly, differing by approximately 25% between the lowest and highest points [36]. The average density of BIP samples is approximately 6% higher (231 ± 9 kg/m^3) compared to LIP (218 ± 4 kg/m^3) [36]. As density increases, compressive strength rises due to a higher ratio of solid material per unit volume and fewer internal air voids [59]. BIP showed a lower percentage of long fibers and a higher percentage of fine particles that also influenced the difference in compression, as panels from the coarse fiber fraction for wood fiber panels are lower than those of panels from the fine fiber fraction [60]. Compared to the LIP material, BIP showed a simultaneous increase in both fine content (from 85.3% to 96.5%, a 13.1% relative increase) [36] and in-plane compressive strength (from 186.4 kPa to 297.8 kPa, a 59.8% relative increase). The increase in specific strength (calculated as the ratio of compressive strength to the fine content percentage) is 41% when comparing LIP to BIP, which may indicate not only the influence of the increased fine content but also the distinctive properties inherent to BIP. However, to build a reliable predictive model, more data points (more fine fraction levels) are needed for correlation.

Test results for force application in the parallel and perpendicular directions do not confirm a specific effect from the loading direction. Although the difference is statistically insignificant ($p > 0.05$), the variance and difference in means are of interest for further study. Since anisotropy was identified during thickness swelling tests, samples were analyzed to observe material behavior before reaching 10% displacement. The compressive strength maximum force σ_{max} was used [61], which represents the absolute breaking point or the peak load the material can sustain before total structural failure occurs.

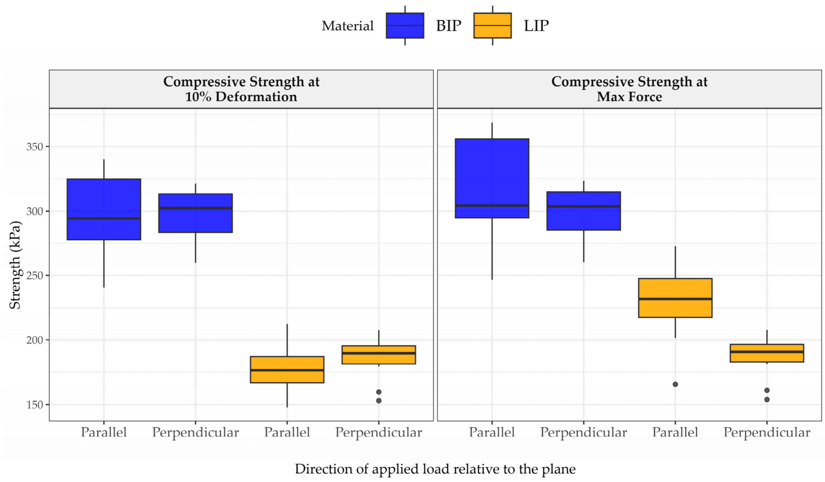

Figure 6. Compressive strength at 10% deformation and maximum force for BIP and LIP made panels in parallel and perpendicular loading directions.

The σ_{max} of BIP remains significantly higher than LIP, depending on the loading direction. Results show that while anisotropy disappeared at 10% deformation, at the moment of peak load, the maximum load-bearing capacity of LIP along the fibers is 25% higher than across the fibers ($p < 0.001$). For BIP, the difference between directions is statistically insignificant ($p > 0.05$). At 10% deformation, structural differences between parallel and perpendicular fibers cease to play a role, and strength equalizes.

For porous materials, this means that the material has entered the compaction stage, where fiber orientation loses its determining influence on compressive strength [62]. High porosity is the main cause of reduced mechanical stability in materials, as voids disrupt the homogeneity of the matrix, which reduces the material's ability to withstand compression [63]. LIP exhibits lower σ_{max} and $\sigma_{10\%}$ and slightly higher sorption capacity than BIP, which may indicate its higher porosity of the material.

Fiber orientation in natural fiber-based composites significantly influences the material's mechanical properties [64]. For composites made using a bamboo bundle layup, the minimum compressive strength is achieved when the fibers are oriented at 90° to the direction of the applied load [65]. In MDF produced via hot pressing, fiber orientation is predominantly through the thickness rather than in-plane, a characteristic that is verified using computed tomography (CT) [66]. In the current study, the fiber orientation was not controlled during the production process, and the orientation can be indirectly explained based on the relative anisotropy at σ_{max}.

Absolute displacement values were taken as an additional measurement to observe different behaviors in various loading directions for the two materials, as shown in Figure 7. The predominant fiber orientation, which affects the mechanical properties of the material [64], was expected from the wet forming used in the current study. In the direction of force toward the formation surface, points are grouped near 10% deformation (3 mm, red line in Figure 7), which is characteristic of the densification process. When composites enter the densification stage under load, pores and cracks gradually compress and decrease, while fibers continue to bear the load. This contributes to a significant increase in the load-bearing capacity of porous composites [62]. For LIP, the material reaches maximum load in the perpendicular force application earlier than in the parallel application, indicating anisotropy. For BIP, the influence of direction is not statistically confirmed; however, the wider confidence ellipse suggests that the structure opposite to the mat formation direction is more porous and non-homogeneous, possibly due to particle size and fiber content percentage.

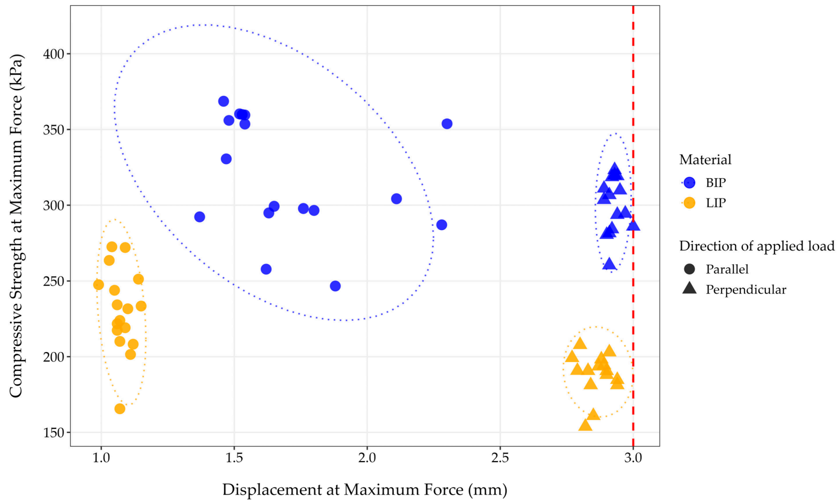

Figure 7. Compressive strength at maximum force versus displacement for BIP and LIP bark insulation panels under parallel and perpendicular loading directions. Red vertical dash line represents 10% of material deformation. Dotted ellipses represent 95% confidence assuming a multidimensional normal distribution.

The parameter combining displacement and maximum load is Young's modulus. No differences were identified for BIP. LIP is more sensitive to fiber direction; its stiffness and maximum strength decrease under perpendicular compression (Table 1). The high variability in mechanical properties is due to the asymmetric density profile across the entire surface of the panels, which is typical for this type of board [67]. The random sampling of specimens captured these local density fluctuations, leading to the observed standard deviation in compressive strength. Bark-based insulation panels (BIP and LIP) show stiffness under compressive loads comparable to that of other bio-based materials. For example, at low densities (≈290 kg/m^3), the apparent Young's modulus for hempcrete ranges from 7 to 25 MPa [68]; for bio-composites made of sunflower stalks and a chitosan binder, the compressive modulus is 25 MPa [69].

Table 1. Mechanical properties of bark-based insulation panels.

Insulation Panel	Direction of Applied Force Relative to the Plane	Young's Modulus (kPa)	Compressive Strength at Maximum Force (kPa)	Compressive Strength at 10% (kPa)	Displacement at Maximum Force (mm)
BIP	Parallel	12.9×10^3 (±2.53)	319.0 (±38.9)	295.0 (±31.3)	1.70 (±0.29)
	Perpendicular	8.94×10^3 (±1.29)	300.0 (±18.4)	298.0 (±18.1)	2.93 (±0.03)
LIP	Parallel	8.52×10^3 (±1.31)	230.0 (±27.3)	178.0 (±17.2)	1.08 (±0.04)
	Perpendicular	4.32×10^3 (±0.49)	188.0 (±14.5)	187.8 (±14.6)	2.86 (±0.05)

±—standard deviation.

For insulation materials made from hardwood species (beech, oak) via thermomechanical pulping, compressive strength is 18 kPa [60]. For non-woody natural insulation, the compressive strength at 10% deformation range for composites made from banana peels [70] ranged between 20 and 170 kPa. Wood fiber panels produced by a dry method from hardwoods (pure birch) showed very low strength, about 11.0 kPa, with pMDI binder [71]. Boards produced with 4% pMDI adhesive using hot-steam or hot-air methods showed compressive strengths over 200 kPa [72]. In the current study, no pressing was applied. The primary strength was achieved during drying, where surface tension forces pull the fibers together as water is removed and hydrogen bonds are formed [73]. Fine

https://doi.org/10.3390/pr14091450

fibers in the hydro-mechanical mass contribute not only to bonding but also to segment activation, a process where initially deformed fiber sections begin to fully support the mechanical load [55].

3.4. Comparison with Other Insulation Materials

The selection of thermal insulation materials for building applications is primarily determined by a combination of climatic conditions, budget constraints, building codes, practical installation considerations, and the physical properties of the material itself [74].

As shown in Table 2, LIP and BIP panels have high compressive strength properties compared to conventional insulation materials, such as EPS, mineral wool, and wood fiber boards. The relatively high compressive strength values for LIP and BIP indicate their potential for use under heavy loads. However, before using the materials in building structures (e.g., under floor loads or as façade insulation boards), additional testing is needed to determine their stability, wear resistance, and flexibility, as well as to address the issue of high water absorption.

The BIP material exhibits extremely high values in water absorption, which is unacceptable for the future use of this material in construction. Therefore, hydrophobization (fiber treatment, bio additives) or constructive protection are necessary [75,76].

Synthetic polystyrene foam (EPS) shows very low water uptake compared to LIP and BIP (<5%), which is a significant advantage for construction applications to maintain high thermal efficiency and ensure long-term durability. However, the structure of expanded polystyrene (EPS) provides low vapor permeability, unlike mineral wool or wood fibers, which have a porous structure and more efficient regulate humidity [77].

Table 2. The comparative characteristics of thermal insulation panels from the current study and traditional insulation materials.

Property	LIP	BIP	EPS (Expanded Polystyrene)	Mineral Wool	Wood Fiber Boards
Thermal conductivity (λ) (W/(m·K))	0.055 [36]	0.057 [36]	0.031–0.046 [78]	0.032–0.045 [79,80]	0.038–0.055 [81,82]
Density (kg/m^3)	218 [36]	231 [36]	8–64 [78,83]	26–150 [80,84]	40–250 [81,82]
Compressive strength at 10% deformation (kPa)	186.40 *	294.85 *	52–250 [83,85]	50.9–142.4 [86]	120–230 [72]
Water absorption after 24h full immersion (%)	57.11 *	320.61 *	<5 [78]	>150 [87]	15–122 [88]

* Current study.

Natural materials have been on the market for a long time, but in most cases, chemically synthesized formaldehyde-based adhesives are still used [89]. As an alternative to such materials, binder-free panels made from wood, agricultural waste or animal wool, produced primarily by hot pressing, as well as less common methods, such as the wet method [29,67], needle-punching [90] and mycelial cultivation, are presented in the literature. The compressive strength of mycelium-based panels can reach 3992 kPa [91], but these values depend on the substrate; for example, for wheat straw and beech sawdust, the compressive strengths are about 17.2–53.3 kPa, which is lower than LIP and BIP panels [92,93]. The mycelium-based insulation material with wood chip substrate shows a moisture absorption of 5.9% at 35% relative humidity, which is comparable to the LIP and BIP values of 5.8 and 5.2%, respectively, at 34% relative humidity [94].

Depending on particle size, binder-free panels made from hot-pressed olive leaf have better water absorption, ranging from 25% to 75% after 24 h of immersion, than BIP panels, but their thickness swelling ranged from 13.66% to 39.35%, which is higher than that of BIP and LIP panels [95].

In insulation panels, the adhesive acts as a structural matrix that binds fibers or particles, ensuring a balance between mechanical strength and water resistance [12]. Therefore, when developing binder-free solutions, it is important to consider that the high water absorption of natural-based binderless insulation panels is an issue that may impact competitiveness compared to traditional options.

4. Conclusions

This study evaluated the thickness swelling, water absorption, hygroscopicity, and mechanical (compressive strength) properties of binderless insulation panels fabricated from the bark of *Robinia pseudoacacia* (black locust, BIP) and *Tilia* spp. (European lime, LIP) using a wet fabrication process. The experimental results demonstrate potential to use bark-based panels as thermal insulation materials.

- Both materials (LIP and BIP) showed similar sorption behavior, reaching approximately 25 and 21.4% moisture content for LIP and BIP accordingly at 93.8% relative humidity.
- Thickness swelling after 24 h of immersion was 4.5% for LIP and 6.0% for BIP. For both materials, the swelling in the perpendicular direction (Z axis) was higher ($p < 0.001$) than in the parallel-to-plane direction (X, Y axes), which indicates the anisotropy of the materials.
- Significant differences between materials in water absorption were observed. After 24 h of immersion, the BIP specimens absorbed significantly more water (320.61%) than LIP (57.11%).

Compressive strength at 10% deformation differed between BIP and LIP specimens ($p < 0.01$), showing 298 ± 18.1 kPa and 188 ± 14.6 kPa accordingly, with the load applied perpendicular to the plane of the specimen.

The studied porous materials have high water absorption compared to EPS, but can be competitive in their mechanical properties (compressive strengths), which are comparable to existing commercial materials on the market (EPS, mineral wool, wood fiber boards).

Future studies should focus on improving material properties, such as reducing moisture absorption, as well as exploring and improving performance characteristics such as biostability, and investigating thermal performance under varying moisture content. To determine the feasibility of producing materials using the wet method without adding an adhesive, it is necessary to conduct a LCA study.

Supplementary Materials: The following supporting information can be downloaded at https://www.mdpi.com/article/10.3390/pr14091450/s1. Table S1: ANOVA results for Thickness Swelling Test; Table S2: Mean results for Thickness Swelling Test; Table S3: Post-hoc results for Thickness Swelling Test; Table S4: ANOVA results for Water Absorption Test; Table S5: Mean results for Water Absorption Test; Table S6: Post-hoc results for Water Absorption Test; Table S7: ANOVA results for Compressive Properties Test; Table S8: Mean results for Compressive Properties Test; Table S9: Post-hoc results for Compressive Properties Test; Table S10: Mean results for Sorption Test.

Author Contributions: Methodology, V.M. and Z.P.; formal analysis, V.M.; investigation, V.M.; writing—original draft preparation, V.M.; writing—review and editing, Z.P.; visualization, V.M.; supervision, Z.P. All authors have read and agreed to the published version of the manuscript.

Funding: This research received no external funding.

Data Availability Statement: The original contributions presented in this study are included in the article/Supplementary Materials. Further inquiries can be directed to the corresponding author.

Conflicts of Interest: The authors declare no conflict of interest.

Abbreviations

The following abbreviations are used in this manuscript:

BIP	Black locust insulation panel
CV	Coefficient of variation

EPS	Expanded polystyrene
GHG	Greenhouse gas
IB	Internal bond
LIP	Lime bark insulation panel
LCA	Life-cycle assessment
MBV	Moisture buffer value
MC	Moisture content
MOE	Modulus of elasticity
MOR	Modulus of rupture
MUF	Melamine–urea–formaldehyde
pH	Potential of hydrogen
pMDI	Polymeric diphenylmethane diisocyanate
RH	Relative humidity
TS	Thickness swelling
UF	Urea–formaldehyde
WA	Water absorption

References

1. Mirzabaev, A.; Bezner Kerr, R.; Hasegawa, T.; Pradhan, P.; Wreford, A.; Cristina Tirado von der Pahlen, M.; Gurney-Smith, H. Severe Climate Change Risks to Food Security and Nutrition. *Clim. Risk Manag.* **2023**, *39*, 100473. [CrossRef]
2. United Nations Environment Programme. Yale Center for Ecosystems + Architecture Building Materials and the Climate: Constructing a New Future. Available online: https://wedocs.unep.org/xmlui/handle/20.500.11822/43293 (accessed on 23 April 2025).
3. United Nations Environment Programme. Global Alliance for Buildings and Construction Not Just Another Brick in the Wall: The Solutions Exist—Scaling Them Will Build on Progress and Cut Emissions Fast. Global Status Report for Buildings and Construction 2024/2025. Available online: https://www.unep.org/resources/report/global-status-report-buildings-and-construction-20242025 (accessed on 9 July 2025).
4. Adamczyk, J.; Dylewski, R. The Impact of Thermal Insulation Investments on Sustainability in the Construction Sector. *Renew. Sustain. Energy Rev.* **2017**, *80*, 421–429. [CrossRef]
5. Eickhoff, H. The Appeal of the Circular Economy Revisited: On Track for Transformative Change or Enabler of Moral Licensing? *Humanit. Soc. Sci. Commun.* **2024**, *11*, 301. [CrossRef]
6. Morandini, M.; Barbu, M.C.; Váňová, R.; Kain, S.; Tippner, J.; Petutschnigg, A.; Kristak, L.; Kain, G.; Sepperer, T.; Schnabel, T. Valorization of Extracted Bark for Particleboard Production: A Life-Cycle Impact Assessment. *Polymers* **2025**, *17*, 925. [CrossRef] [PubMed]
7. Razi, N.; Ansari, R. A Prediction-Based Model to Optimize Construction Programs: Considering Time, Cost, Energy Consumption, and CO_2 Emissions Trade-Off. *J. Clean. Prod.* **2024**, *445*, 141164. [CrossRef]
8. Ali, A.; Issa, A.; Elshaer, A. A Comprehensive Review and Recent Trends in Thermal Insulation Materials for Energy Conservation in Buildings. *Sustainability* **2024**, *16*, 8782. [CrossRef]
9. Ye, F.; Wei, H.; Xiao, Y.; Berardi, U.; Quaranta, G.; Demartino, C. Bio-Based Insulation Materials in Sustainable Constructions: A Review of Environmental, Thermal and Acoustic Insulation, Durability, and Mechanical Performances. *Renew. Sustain. Energy Rev.* **2025**, *223*, 115872. [CrossRef]
10. Schulte, M.; Lewandowski, I.; Pude, R.; Wagner, M. Comparative Life Cycle Assessment of Bio-Based Insulation Materials: Environmental and Economic Performances. *GCB Bioenergy* **2021**, *13*, 979–998. [CrossRef]
11. Asfaw, N.T.; Absi, R.; Labouda, B.A.; EL Abbassi, I. Assessment of the Thermal and Mechanical Properties of Bio-Based Composite Materials for Thermal Insulation: A Review. *J. Build. Eng.* **2024**, *97*, 110605. [CrossRef]
12. Pawłosik, D.; Cebrat, K.; Brzezicki, M. Exploring Advancements in Bio-Based Composites for Thermal Insulation: A Systematic Review. *Sustainability* **2025**, *17*, 1143. [CrossRef]
13. Carcassi, O.B.; Habert, G.; Malighetti, L.E.; Pittau, F. Material Diets for Climate-Neutral Construction. *Environ. Sci. Technol.* **2022**, *56*, 5213–5223. [CrossRef]
14. Fischer, H.; Korjenic, A. Hygrothermal Performance of Bio-Based Exterior Wall Constructions and Their Resilience under Air Leakage and Moisture Load. *Buildings* **2023**, *13*, 2650. [CrossRef]
15. Cosentino, L.; Fernandes, J.; Mateus, R. A Review of Natural Bio-Based Insulation Materials. *Energies* **2023**, *16*, 4676. [CrossRef]
16. Cintura, E.; Nunes, L.; Molari, L.; Bettuzzi, M.; Morigi, M.P.; Brancaccio, R.; Faria, P. Hygroscopicity and Morphology of Bio-Based Boards—The Influence of the Formulation. *Appl. Sci.* **2024**, *14*, 873. [CrossRef]

17. Palumbo, M.; Lacasta, A.M.; Holcroft, N.; Shea, A.; Walker, P. Determination of Hygrothermal Parameters of Experimental and Commercial Bio-Based Insulation Materials. *Constr. Build. Mater.* **2016**, *124*, 269–275. [CrossRef]
18. Boro, D.; Kieno, P.F.; Ouedraogo, E. Experimental Study of the Thermal and Mechanical Properties of Compressed Earth Blocks Stabilized with Sawdust According to the Rates for the Thermal Insulation of a Building. *Int. J. Constr. Eng. Manag.* **2017**, *6*, 103–109. [CrossRef]
19. Mlhem, A.; Teklebrhan, T.; Bokuretsion, E.; Abu-Jdayil, B. Development of Sustainable Thermal Insulation Based on Bio-Polyester Filled with Date Pits. *J. Bioresour. Bioprod.* **2024**, *9*, 74–89. [CrossRef]
20. Wu, Y.; Chen, X.; Liao, Q.; Xiao, N.; Li, Y.; Huang, Z.; Xie, S. Development of Binderless Fiberboard from Poplar Wood Residue with *Trametes hirsuta*. *Chemosphere* **2024**, *362*, 142638. [CrossRef]
21. Supriyadi, D.; Damayanti, D.; Veigel, S.; Hansmann, C.; Gindl-Altmutter, W. Unlocking the Potential of Tree Bark: Review of Approaches from Extractives to Materials for Higher-Added Value Products. *Mater. Today Sustain.* **2025**, *29*, 101074. [CrossRef]
22. Pásztory, Z.; Mohácsiné, I.R.; Gorbacheva, G.; Börcsök, Z. The Utilization of Tree Bark. *Bioresources* **2016**, *11*, 7859–7888. [CrossRef]
23. Kress, O. The Use of Bark for Paper Specialties. *Ind. Eng. Chem.* **1916**, *8*, 883–886. [CrossRef]
24. Muszynski, Z.; Dobbin Mcnatt, J. Investigations on the Use of Spruce Bark in the Manufacture of Particleboard in Poland. *For. Prod. J.* **1984**, *34*, 28–35.
25. Gupta, G.; Yan, N.; Feng, M.W. Effects of Pressing Temperature and Particle Size on Bark Board Properties Made from Beetle-Infested Lodgepole Pine (*Pinus contorta*) Barks. *For. Prod. J.* **2011**, *61*, 478–488. [CrossRef]
26. Kain, G.; Barbu, M.C.; Hinterreiter, S.; Richter, K.; Petutschnigg, A. Using Bark as a Heat Insulation Material. *Bioresources* **2013**, *8*, 3718–3731. [CrossRef]
27. Oktoberyani Christy, E.; Hadi Sumarlan, S.; Soehardjono, A. Gelam Wood Particleboards. *Bioresources* **2020**, *15*, 7390–7403. [CrossRef]
28. Medved, S.; Tudor, E.M.; Barbu, M.C.; Young, T.M. Thermal Conductivity of Different Bio-Based Insulation Materials. *Les/Wood* **2021**, *70*, 73–82. [CrossRef]
29. Gößwald, J.; Barbu, M.C.; Petutschnigg, A.; Tudor, E.M. Binderless Thermal Insulation Panels Made of Spruce Bark Fibres. *Polymers* **2021**, *13*, 1799. [CrossRef] [PubMed]
30. Bakatovich, A.; Bakatovich, N.; Silva, A.; Gaspar, F. Thermal Insulation Materials Based on Eucalyptus Bark Fibres. *Constr. Build. Mater.* **2024**, *449*, 138559. [CrossRef]
31. Kain, G.; Lienbacher, B.; Barbu, M.C.; Richter, K.; Petutschnigg, A. Larch (*Larix decidua*) Bark Insulation Board: Interactions of Particle Orientation, Physical-Mechanical and Thermal Properties. *Eur. J. Wood Wood Prod.* **2018**, *76*, 489–498. [CrossRef]
32. Kain, G.; Güttler, V.; Barbu, M.C.; Petutschnigg, A.; Richter, K.; Tondi, G. Density Related Properties of Bark Insulation Boards Bonded with Tannin Hexamine Resin. *Eur. J. Wood Wood Prod.* **2014**, *72*, 417–424. [CrossRef]
33. Christy, E.O.; Soemarno; Sumarlan, S.H.; Soehardjono, A. Binderless Bark Particleboard Made from Gelam (*Melaleuca viridiflora* Sol. Ex Gaertn.) Bark Waste: The Effect of the Pressing Temperature on Its Mechanical and Physical Properties. *Bioresources* **2021**, *16*, 4171–4199. [CrossRef]
34. Kain, G.; Tudor, E.M.; Barbu, M.C. Bark Thermal Insulation Panels: An Explorative Study on the Effects of Bark Species. *Polymers* **2020**, *12*, 2140. [CrossRef] [PubMed]
35. Bossu, J.; Moreau, J.; Delisée, C.; Le Moigne, N.; Corn, S.; Sonnier, R.; Viretto, A.; Beauchêne, J.; Clair, B. Revealing the Potential of Waste Fibers from Timber Production and Clearings for the Development of Local Bio-Based Insulation Fiberboards in French Guiana. *Waste Biomass Valorization* **2023**, *14*, 4281–4295. [CrossRef]
36. Mialeshka, V.; Kowaluk, G.; Pásztory, Z. Sustainable Insulation Panels Made of Tree Bark Fibers: Thermal and Fire Performance. *Forests* **2025**, *17*, 26. [CrossRef]
37. *ISO 12571*; Hygrothermal Performance of Building Materials and Products—Determination of Hygroscopic Sorption Properties. International Organization for Standardization: Geneva, Switzerland, 2021.
38. *EN 317*; Particleboards Thickness Swelling Test Method Guide. European Standard: Brussels, Belgium, 1993.
39. *ASTM C1763-20*; Standard Test Method for Water Absorption by Immersion of Thermal Insulation Materials. ASTM International: West Conshohocken, PA, USA, 2020. [CrossRef]
40. *EN 826*; Thermal Insulating Products for Building Applications. European Standard: Brussels, Belgium, 2013.
41. Keaton, J.R. Young's Modulus. In *Encyclopedia of Engineering Geology*; Springer: Berlin/Heidelberg, Germany, 2018; pp. 955–956. [CrossRef]
42. *ISO 8301*; Thermal Insulation, Determination of Steady-State Thermal Resistance and Related Properties, Heat Flow Meter Apparatus. International Organization for Standardization: Geneva, Switzerland, 1991.
43. *EN 12667:2002*; Thermal Performance of Building Materials and Products—Determination of Thermal Resistance by Means of Guarded Hot Plate and Heat Flow Meter Methods—Products of High and Medium Thermal Resistance. European Committee for Standardization: Brussels, Belgium, 2002.

44. Pazireh, S.; Mirazimzadeh, S.E.; Urbanic, J. Application of Linear Mixed-Effects Model, Principal Component Analysis, and Clustering to Direct Energy Deposition Fabricated Parts Using FEM Simulation Data. *Materials* **2024**, *17*, 5127. [CrossRef]
45. Kielsgaard, K. *General Rights Sorption Isotherms A Catalogue*; Technical University of Denmark: Lyngby, Denmark, 1986.
46. Petcu, C.; Hegyi, A.; Stoian, V.; Dragomir, C.S.; Ciobanu, A.A.; Lăzărescu, A.V.; Florean, C. Research on Thermal Insulation Performance and Impact on Indoor Air Quality of Cellulose-Based Thermal Insulation Materials. *Materials* **2023**, *16*, 5458. [CrossRef]
47. Palumbo, M.; Lacasta, A.M.; Giraldo, M.P.; Haurie, L.; Correal, E. Bio-Based Insulation Materials and Their Hygrothermal Performance in a Building Envelope System (ETICS). *Energy Build.* **2018**, *174*, 147–155. [CrossRef]
48. Ranefjärd, O.; Strandberg-de Bruijn, P.B.; Wadsö, L. Hygrothermal Properties and Performance of Bio-Based Insulation Materials Locally Sourced in Sweden. *Materials* **2024**, *17*, 2021. [CrossRef] [PubMed]
49. O'Hegarty, R.; Amedeo, G.; Kinnane, O. The Impact of Compromised Insulation on Building Energy Performance. *Energy Build.* **2024**, *316*, 114337. [CrossRef]
50. Rode, C.; Peuhkuri, R.; Time, B.; Svennberg, K.; Ojanen, T. Moisture Buffer Value of Building Materials. *J. ASTM Int.* **2007**, *4*, 100369. [CrossRef]
51. Wildman, J.; Shea, A.; Cascione, V.; Henk, D. Mould Susceptibility of Bio-Based Insulation Materials in Modern Construction. *Npj Mater. Degrad.* **2026**, *10*, 29. [CrossRef]
52. Tupciauskas, R.; Orlovskis, Z.; Blums, K.T.; Liepins, J.; Berzins, A.; Pavlovics, G.; Andzs, M. Mold Fungal Resistance of Loose-Fill Thermal Insulation Materials Based on Processed Wheat Straw, Corn Stalk and Reed. *Polymers* **2024**, *16*, 562. [CrossRef] [PubMed]
53. Zhang, H.; Wang, H.; Liu, Y.; Tao, L.; Qu, J.; Liang, C. Experimental Study on Particle Settling in Fiber-Containing Non-Newtonian Fluids. *Processes* **2025**, *13*, 2542. [CrossRef]
54. Khatmullina, L.; Chubarenko, I. Thin Synthetic Fibers Sinking in Still and Convectively Mixing Water: Laboratory Experiments and Projection to Oceanic Environment. *Environ. Pollut.* **2021**, *288*, 117714. [CrossRef] [PubMed]
55. Vainio, A.K.; Paulapuro, H. Interfiber Bonding and Fiber Segment Activation in Paper. *Bioresources* **2007**, *2*, 442–458. [CrossRef]
56. *EN 622-4*; Fibreboards—Specifications—Part 4: Requirements. European Standard: Brussels, Belgium, 2019.
57. Nociar, M.; Pipíška, T.; Bekhta, P.; Král, P. Effect of Wood Species, Bark Particle Size, and Adhesive Type on the Properties of Bark-Based Boards. *BioResources* **2025**, *20*, 4044–4067. [CrossRef]
58. Alsubari, S.; Zuhri, M.Y.M.; Sapuan, S.M.; Ishak, M.R.; Ilyas, R.A.; Asyraf, M.R.M. Potential of Natural Fiber Reinforced Polymer Composites in Sandwich Structures: A Review on Its Mechanical Properties. *Polymers* **2021**, *13*, 423. [CrossRef]
59. Affan, H.; El Haddaji, B.; Ajouguim, S.; Khadraoui, F. Comparative Analysis of Bio-Based Insulation Materials with Low-Carbon Binders: Mechanical, Hygrothermal, and Durability Performance. *Case Stud. Constr. Mater.* **2025**, *22*, e04915. [CrossRef]
60. Brinker, S.; Ahrens, C.; Gurnik, M.; Mayer, A.K.; Mai, C. Influence of Screened Fibre Fractions on the Properties of Insulation Panels Made of Different Wood Species. *Wood Mater. Sci. Eng.* **2025**, *21*, 751–761. [CrossRef]
61. Cárdenas-Oscanoa, A.J.; Tayo, L.T.; Nayaka, D.S.; Euring, M. Low-Density Wood-Fiber Insulation Boards Produced with Canola Isolated-Protein Based as a Binder. *J. Nat. Fibers* **2025**, *22*, 2578609. [CrossRef]
62. Wu, M.; Xu, Z.; Gao, Y. Compression Behaviour of Porous Mof/Ti-12Nb-18Zr Composite with Short Mo Fibers. *J. Alloys Compd.* **2024**, *980*, 173577. [CrossRef]
63. Touil, M.; Rahmoun, O.; El Harti, K.; Saadani, R.; Rahmoune, M. Bio-Based Construction Composites for Improved Thermal Efficiency: Properties, Methods, and Performance. *Clean. Waste Syst.* **2026**, *14*, 100499. [CrossRef]
64. Prasanthi, P.P.; Ramacharyulu, D.A.; Babu, K.S.; Madhav, V.V.V.; Chaitanya, C.S.; Saxena, K.K.; Revathi, V.; Abduvalieva, D.; Bandhu, D. Role of Fiber Orientation and Design on Thermal and Mechanical Properties of Natural Composite. *Int. J. Interact. Des. Manuf. IJIDeM* **2024**, *19*, 1383–1393. [CrossRef]
65. Yun, H.; Chen, R.; Wu, Y.; Xu, J.; Li, X.; Li, T.; Li, X. The Effect of Loading Orientation on the Compressive Bearing Behavior of Bamboo Engineering Composites. *Ind. Crops Prod.* **2025**, *237*, 122207. [CrossRef]
66. Sliseris, J.; Andrä, H.; Kabel, M.; Wirjadi, O.; Dix, B.; Plinke, B. Estimation of Fiber Orientation and Fiber Bundles of MDF. *Mater. Struct.* **2015**, *49*, 4003–4012. [CrossRef]
67. Göβwald, J.; Barbu, M.C.; Nemec, M.; Igaz, R.; Adamcik, L.; Kristak, L.; Tudor, E.M. Innovative Porous Panels Made from Alpine Tree Bark-Fibre Bundles for Enhanced Acoustic and Thermal Insulation. *Wood Mater. Sci. Eng.* **2025**, *21*, 778–789. [CrossRef]
68. Elfordy, S.; Lucas, F.; Tancret, F.; Scudeller, Y.; Goudet, L. Mechanical and Thermal Properties of Lime and Hemp Concrete ("Hempcrete") Manufactured by a Projection Process. *Constr. Build. Mater.* **2008**, *22*, 2116–2123. [CrossRef]
69. Mati-Baouche, N.; De Baynast, H.; Lebert, A.; Sun, S.; Lopez-Mingo, C.J.S.; Leclaire, P.; Michaud, P. Mechanical, Thermal and Acoustical Characterizations of an Insulating Bio-Based Composite Made from Sunflower Stalks Particles and Chitosan. *Ind. Crops Prod.* **2014**, *58*, 244–250. [CrossRef]
70. Trobiani Di Canto, J.A.; Malfait, W.J.; Wernery, J. Turning Waste into Insulation—A New Sustainable Thermal Insulation Board Based on Wheat Bran and Banana Peels. *Build. Environ.* **2023**, *244*, 110740. [CrossRef]

71. Imken, A.A.P.; Kraft, R.; Mai, C. Production and Characterisation of Wood-Fibre Insulation Boards (WFIB) from Hardwood Fibres and Fibre Blends. *Wood Mater. Sci. Eng.* **2022**, *17*, 802–808. [CrossRef]
72. Euring, M.; Kirsch, A.; Kharazipour, A. Hot-Air/Hot-Steam Process for the Production of Laccase-Mediator-System Bound Wood Fiber Insulation Boards. *Bioresources* **2015**, *10*, 3541–3552. [CrossRef]
73. Zhang, D.; Zhang, A.; Xue, L. A Review of Preparation of Binderless Fiberboards and Its Self-Bonding Mechanism. *Wood Sci. Technol.* **2015**, *49*, 661–679. [CrossRef]
74. Al-Homoud, M.S. Performance Characteristics and Practical Applications of Common Building Thermal Insulation Materials. *Build. Environ.* **2005**, *40*, 353–366. [CrossRef]
75. Mokhothu, T.H.; John, M.J. Bio-Based Coatings for Reducing Water Sorption in Natural Fibre Reinforced Composites. *Sci. Rep.* **2017**, *7*, 13335. [CrossRef]
76. Prome, F.S.; Hossain, M.F.; Rana, M.S.; Islam, M.M.; Ferdous, M.S. Different Chemical Treatments of Natural Fiber Composites and Their Impact on Water Absorption Behavior and Mechanical Strength. *Hybrid Adv.* **2025**, *8*, 100379. [CrossRef]
77. Ducoulombier, L.; Lafhaj, Z. Comparative Study of Hygrothermal Properties of Five Thermal Insulation Materials. *Case Stud. Therm. Eng.* **2017**, *10*, 628–640. [CrossRef]
78. Gnip, I.; Vejelis, S.; Vaitkus, S. Thermal Conductivity of Expanded Polystyrene (EPS) at 10 °C and Its Conversion to Temperatures within Interval from 0 to 50 °C. *Energy Build.* **2012**, *52*, 107–111. [CrossRef]
79. Lu, G. Study on the Properties of Rock Wool for External Thermal Insulation of Buildings under the Soaking and Hot & Humid Conditions. *J. Phys. Conf. Ser.* **2020**, *1622*, 012006. [CrossRef]
80. Loboda, B.; Szurman, F. Thermal Conductivity Coefficient Research on Mineral Wool After Partial Immersion in Water and Drying to Constant Mass. *IOP Conf. Ser. Mater. Sci. Eng.* **2019**, *471*, 022022. [CrossRef]
81. Troppová, E.; Švehlík, M.; Tippner, J.; Wimmer, R. Influence of Temperature and Moisture Content on the Thermal Conductivity of Wood-Based Fibreboards. *Mater. Struct.* **2014**, *48*, 4077–4083. [CrossRef]
82. O'Brien, L.; Li, L.; Friess, W.; Snow, J.; Herzog, B.; O'Neill, S. Review of Bio-Based Wood Fiber Insulation for Building Envelopes: Characteristics and Performance Assessment. *Energy Build.* **2025**, *328*, 115114. [CrossRef]
83. Veiseh, S.; Yousefi, A.A. Compressive Behavior and Thermal Conductivity-Density Correlation of Expanded Polystyrene Thermal Insulators. *Iran. Polym. J.* **2021**, *30*, 849–854. [CrossRef]
84. Ablaoui, E.M.; Malendowski, M.; Szymkuc, W.; Pozorski, Z. Determination of Thermal Properties of Mineral Wool Required for the Safety Analysis of Sandwich Panels Subjected to Fire Loads. *Materials* **2023**, *16*, 5852. [CrossRef]
85. Ramli Sulong, N.H.; Mustapa, S.A.S.; Abdul Rashid, M.K. Application of Expanded Polystyrene (EPS) in Buildings and Constructions: A Review. *J. Appl. Polym. Sci.* **2019**, *136*, 47529. [CrossRef]
86. Buska, A.; Mačiulaitis, R. The Compressive Strength Properties of Mineral Wool Slabs: Influence of Structure Anisotropy and Methodical Factors. *J. Civ. Eng. Manag.* **2007**, *13*, 97–106. [CrossRef]
87. Akkuş, M. Hybrid Composite Board Produced from Wood and Mineral Stone Wool Fibers. *Bioresources* **2022**, *17*, 6245–6261. [CrossRef]
88. Snow, J.; Herzog, B.; O'brien, L.; Li, L. Characterization of Wood Fiber Insulation for the Development of Wood Fiber-Insulated Panels (WIPs) for Use in Building Envelope. *Bioresources* **2024**, *19*, 6142–6159. [CrossRef]
89. Ćehić, M.; Talić, H.; Omer, S.E. Eco-Friendly Adhesives for Wood-Based Composite Production. *IOP Conf. Ser. Mater. Sci. Eng.* **2023**, *1298*, 012013. [CrossRef]
90. Kicińska-Jakubowska, A.; Broda, J.; Zimniewska, M.; Bączek, M.; Mańkowski, J. Effect of Blend Composition on Barrier Properties of Insulating Mats Produced from Local Wool and Waste Bast Fibres. *Materials* **2023**, *16*, 459. [CrossRef] [PubMed]
91. Grenon, V.; Maref, W.; Ouellet-Plamondon, C.M. Multi-Property Characterization of an Experimental Material Composed of Pleurotus Ostreatus Mycelium and Ash Wood Chips Compared with Glass Wool and Hemp Wool. *Constr. Build. Mater.* **2023**, *409*, 133941. [CrossRef]
92. Dias, P.P.; Jayasinghe, L.B.; Waldmann, D. Investigation of Mycelium-Miscanthus Composites as Building Insulation Material. *Results Mater.* **2021**, *10*, 100189. [CrossRef]
93. Kuştaş, S.; Gezer, E.D. Physical and Mechanical Properties of Mycelium-Based Insulation Materials Produced from Desilicated Wheat Straws—Part A. *Bioresources* **2024**, *19*, 1330–1347. [CrossRef]
94. Wimmers, G.; Klick, J.; Tackaberry, L.; Zwiesigk, C.; Egger, K.; Massicotte, H. Fundamental Studies for Designing Insulation Panels from Wood Shavings and Filamentous Fungi. *BioResources* **2019**, *14*, 5506–5520. [CrossRef]
95. Ferrandez-Garcia, A.; Ferrandez-Garcia, M.T.; Ortuño, T.G.; Mata-Cabrera, F.; Ferrandez-Villena, M. Analysis of the Manufacturing Variables of Binderless Panels Made of Leaves of Olive Tree (*Olea europaea* L.) Pruning Waste. *Agronomy* **2021**, *12*, 93. [CrossRef]

https://doi.org/10.3390/pr14091450